Volume 292, number 1,2, 223–228 FEBS 10355 November 1991

ADONIS 0014579391010614

Map of chartreusin and elsamicin binding sites on DNA

Xavier Salas and José Portugal

Departamento de Bioquímica y Fisiología, Universidad de Barcelona, Barcelona, Spain

Received 21 June 1991; revised version received 6 September 1991

Three DNA restriction fragments designated tyrT, 102-mer and 70-mer, have been used as substrates for footprinting studies using DNase I in the presence of the structurally similar antibiotics chartreusin and elsamicin A. The sequence-selective binding sites of the antibiotics can be mapped in regions which are rich in guanine+cytosine. Chartreusin and elsamicin appear to recognize and bind preferentially to sequences containing a CpG step. Regions containing a TpG step also seem to be a good binding site. The binding of elsamicin to these sites appears to be more concentration-dependent. A comparative analysis is performed of the sizes and locations of the different binding sites, aimed to infer whether the different biological effects of chartreusin and elsamicin A can be correlated to differences in their sequence-selective binding to DNA.

Antibiotic–DNA binding; Footprinting; Chartreusin; Elsamicin A

1. INTRODUCTION

Chartreusin and elsamicin A are two structurally related antibiotics (see Fig. 1) containing the common aglycone chartarin but different sugar moieties [1–4]. Although chartreusin is active against a number of mouse tumours [5] it is an improbable candidate for clinical trials because of its water insolubility and poor pharmacokinetic profile [3,5]. Elsamicin A, which is much more water-soluble especially under acidic conditions, is several times more potent in a number of murine tumours [2], and it is at present undergoing Phase I clinical trials [6].

Chartreusin (Fig. 1) is known to induce strand scission in a reducing environment and to inhibit relaxation of negatively superhelical DNA [7,8]. Although direct interaction with DNA is believed to be central to the mechanism by which chartreusin acts [3,7,8], the investigations aimed at detecting possible base-sequence selectivity in the binding of this antibiotic to DNA have yielded conflicting results [3]. It appears to bind cooperatively to A+T and G+C polymers but not to calf-thymus DNA, reflecting some affinity for alternating pyrimidine–purine base pairs [3]. Resulting on the sequence-specific binding of elsamicin A (Fig. 1) to DNA are more scarce. It has been observed that elsamicin produces extensive DNA breakage in intact cells but not in pure DNA in vitro [9]. The possible site or sequence specificity of the elsamicin-DNA interaction remains undefined.

In order to clarify the sequence specificity of the DNA interaction with chartreusin and elsamicin we have employed the technique of DNase I footprinting (reviewed in [10]) to locate the precise binding sites for both antibiotics. Our results provide the clearest experimental evidence to date that both chartreusin and elsamicin A recognize and bind preferentially to the sequence CpG, most probably within a longer sequence, despite the differences found in their chemical structure (see Fig. 1). Nonetheless, some differences are observed in the behaviour of the antibiotics and the size of the binding sites.

Correspondence address: J. Portugal, Departamento de Bioquímica y Fisiología, Universidad de Barcelona, Facultad de Química, Diagonal 647, 08028 Barcelona, Spain. Fax: (34) (3) 490 14 83.

2. MATERIALS AND METHODS

2.1. *Antibiotics*

Chartreusin (U-7257) was a gift from Dr. W.C. Krueger (The Upjohn Co., Kalamazoo, USA). Elsamicin A (BMY-28090) was kindly provided by Bristol-Myers Co. (Wallingford, USA). 1 mM stock solutions of each antibiotic were prepared by direct weighing and dissolved in dimethylsulphoxide (DMSO). Fresh diluted solutions were prepared from the stocks diluted in 10 mM Tris-HCl, pH 7.5 containing 10 mM NaCl.

2.2. *DNA substrates*

The 160-base pair tyrT fragment from *E. coli* (Fig. 2), containing a tRNA promoter, was isolated and labelled at the 3'-end of its lower (Crick) strand using reverse transcriptase and [α-^{32}P]dATP [11–13]. The 102-mer and 70 base-pair fragments from pBR322 (Fig. 2), were cut out of the plasmid and labelled with [α-^{32}P]dATP as described elsewhere [14,15].

2.3. *DNase I footprinting*

Samples of the labelled DNA fragments (9 pmol in base pairs) were incubated with an appropriate antibiotic solution, at 37°C for 30 min, to give concentrations between 1 and 100 μM of chartreusin or elsamicin A, so the final DMSO concentration was below 10%. These solvent concentrations do not alter the footprinting experiments significantly [16].

DNase I was purchased from Boehringer Mannheim and prepared as a 7200 units/ml stock solution in 0.15 M NaCl containing 1 mM

$MgCl_2$. It was stored at −20°C and diluted to working concentration immediately before use.

DNase I footprints were performed as previously described [12–14]. The products of the nuclease digestion were analysed on 0.3 mm polyacrylamide gels (8% for the tyrT DNA fragment; 12% for the 70-mer and 102-mer) containing Tris-borate-EDTA buffer, pH 8.3.

2.4. *Dimethyl sulphate modification*

After incubation of the DNA fragments together with the antibiotics, dimethylsulphate modification was performed basically as described in [16].

2.5. *Densitometry and analysis*

Autoradiographs from the DNase I footprinting experiments were analysed using a Joyce-Loebl NR-III-CS microdensitometer to produce profiles from which the intensity of each band was measured. Band intensities were transformed into values for the fractional cleavage (f)=A_i/A_t, where A_i is the area under band i and A_t is the sum of the areas under all bands in any gel lane [12–14].

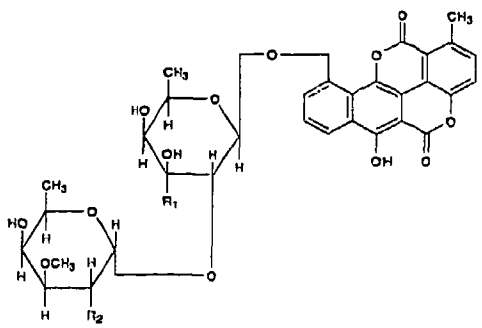

CHARTREUSIN: R_1= -H; R_2= -OH

ELSAMICIN A: R_1= $-CH_3$; R_2= $-NH_3^+$

Fig. 1. Chemical structures of chartreusin and elsamicin A.

3. RESULTS

Typical DNase I digestion patterns for the 160-base-pair tyrT DNA fragment in the presence of three different elsamicin concentrations and 30 μM chartreusin are displayed in Fig. 3. Each gel lane contains about 100 bands that can be satisfactorily resolved. The densitometric analysis of these bands produces the differential cleavage plots shown in Fig. 4. It is immediately apparent that the cleavage pattern in the presence of both antibiotics is different from that of the DNA alone. Regions protected from digestion are readily apparent near positions 35, 55, 70, 95 and 115. It is also evident that the rate of cleavage at certain bonds is strongly enhanced compared with the control.

We examined the effect on the digestion pattern of several antibiotic concentrations in the range between 1 and 100 μM, the patterns remained essentially constant for chartreusin, while it appears that elsamicin A concentrations higher than about 20 μM render slightly larger footprints and an increase, in all cases, in the extent of the protection pattern as displayed in Fig. 4. Moreover, a clear difference is observed, even at lower concentrations of elsamicin, in some regions as for example around position 35 where the protected zone is always larger than for chartreusin. That the chartreusin footprints are not as impressive as those of elsamicin is somewhat puzzling and probably arises from differences in the binding characteristics of the two compounds. Since these sites are more concentration dependent than the CG-zones (see Fig. 3) we think that they might represent a weaker binding site, since DNase I is considered to be a good probe to detect such binding

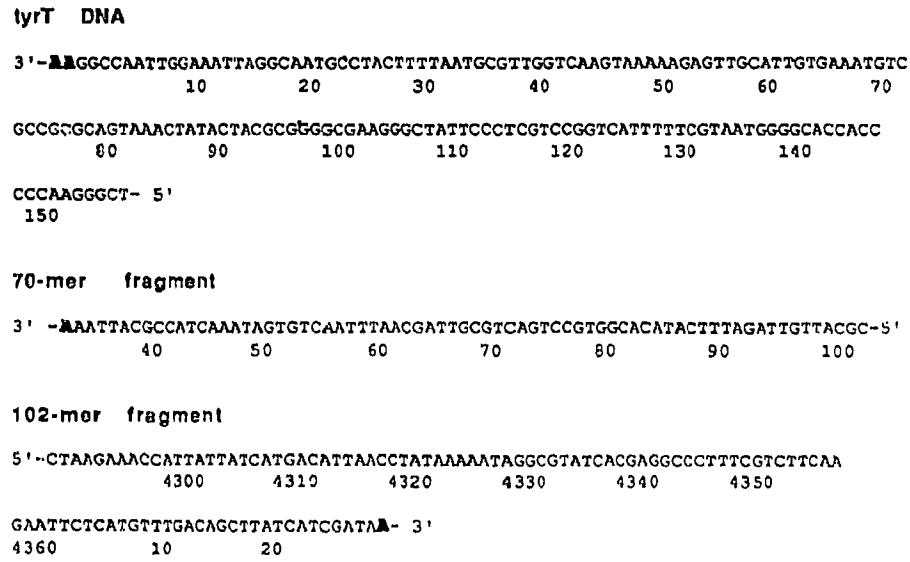

Fig. 2. Sequences of the DNA fragments used in the footprinting experiments. Only the strand bearing the radioactive label (outlined) is shown.

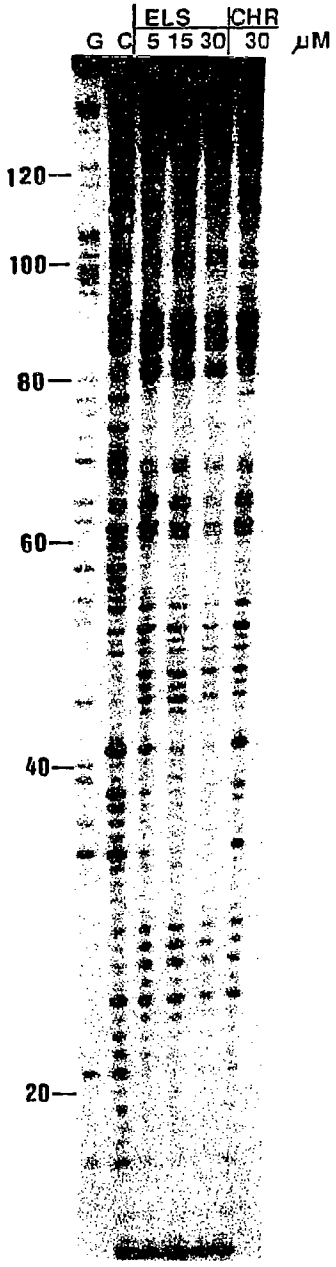

Fig. 3. DNase I footprinting of elsamicin A (ELS: 5 μM, 15 μM and 30 μM) and chartreusin (CHR: 30 μM) bound to the 160 bp duplex tyrT DNA (9 pmol in base pairs) whose sequence is shown in Fig. 2. Digestions were performed for 2 min. The Crick (bottom) strand is displayed. A track labelled G represents a dimethylsulphate-piperidine marker specific for guanine. The samples were run together with a control (C) to which no drug had been added.

sites [10]. It is well known that a zone protected from DNase I attack cannot always be correlated in a straightforward manner with the real binding site size [17]. However, because these differences are observed with two closely related antibiotics it is reasonable to suppose that a detailed analysis of the protected regions can give clues on any difference between the sequence-selective binding sites for chartreusin and elsamicin A.

In order to investigate the effects of chartreusin and elsamicin on DNA, as well as to gain more information to compare their binding sites, we performed further footprinting experiments using 70 and 102 base-pair fragments derived from pBR322. Illustrated in Fig. 5 are electrophoretic patterns determined in the presence of each antibiotic. Differential cleavage plots calculated from the data are represented in Fig. 6. Once again, clear regions of blockage are observed, which are even more apparent than on the tyrT DNA, for example around positions 4345 (102-mer) or 70 (70-mer). As for the tyrT DNA, all these protected regions are mostly GC-rich, thus we can state with confidence that chartreusin and elsamicin bind to DNA regions containing G+C base pairs. The DNA region around the position 50 in the 70-mer DNA is another clear example of the binding of elsamicin to TpG steps (Figs. 2 and 5). This region behaves as a weaker binding site for chartreusin. The size of the regions protected from DNase I cleavage ranges from a minimum of four base pairs (around position 105 in the tyrT DNA) a value near that of the exclusion parameter of chartreusin [3], to 11 base pairs (around position 40 in the same fragment). These values are even more impressive when the elsamicin concentration is raised over 30 μM. We also found (data not shown) that the presence of chartreusin and elsamicin does not significantly alter the guanine-specific dimethylsulphate-piperidine cleavage of the tyrT and 102-mer DNAs. Since this reaction is particularly sensitive to ligand blockage in the major groove, we conclude that chartreusin and elsamicin would probably interact with DNA throughout the minor groove, a common property displayed by most of the intercalating agents [10].

4. DISCUSSION

Chartreusin and elsamicin A produce distinctly altered patterns of DNase I digestion (Figs. 3 and 5). In general, the regions protected by elsamicin from the enzyme attack are larger than those seen for chartreusin. The data presented in this paper provide the basis for a detailed comparison between the effects of the two antibiotics. The first, and main, conclusion is that they bind preferentially to (and protect from DNase I cleavage) regions containing adjacent guanine+cytosine base pairs. The precise sequence appears to be a pyrimidine–purine arrangement (probably CpG). Chartreusin and elsamicin A seem to present a less pronounced sequence specificity than other intercalators as actinomycin D [13] or echinomycin [12]. The presence of a CG tract as a binding site for chartreusin is not at variance with a study performed using restriction enzymes, which suggests that it binds to CGC regions [8]. A comparison of Figs. 3 and 5 shows that the binding sites are larger for elsamicin. Since the differences between these antibiotics reside in the disaccharide moiety

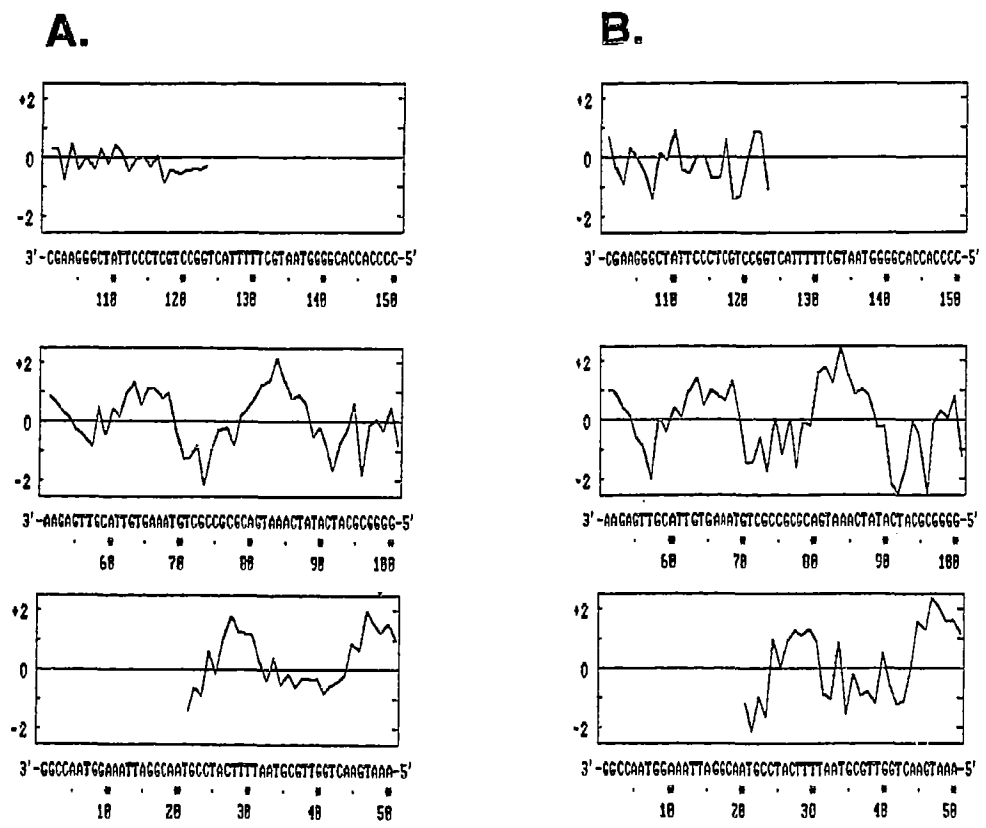

Fig. 4. Differential cleavage plots for the difference in susceptibility of the tyrT fragment (bottom strand) to DNase I attack in the presence of: 30 μM chartreusin (A), and 15 μM elsamicin (B). The ordinate scale is in units of $\ln(f_a)-\ln(f_c)$ where f_c is the fractional cleavage in a control experiment and f_a is the fractional cleavage of the same bond in the presence of antibiotic. Negative values on the ordinate indicate protection by the bound antibiotic, positive values indicate enhanced cleavage.

(see Fig. 1) we tentatively considered that the sizes possibly reflected that the binding site for elsamicin could be a quadruplet site to favour interactions between the charged amino sugar and the first base (of four) at the 5'-end of the binding site. Alternatively, the extra hydrogen bond might account for the binding of elsamicin to TpG (possibly as 5'pyrTG3' triplets). Nevertheless, it could be considered that the larger footprints reflect a major distortion of the DNA substrate produced by elsamicin binding. An indirect way to detect the effect of bound ligands on the DNA structure is to consider the enhancements observed in the footprinting gels and in the differential plots. The enhancements produced by elsamicin binding are more potent than those induced by chartreusin, yet the differences seem too small to conclude that the footprint sizes are a direct consequence of a bigger distortion of the DNA double helix after elsamicin binding. The clear concentration-dependent response produced by elsamicin in contrast with chartreusin was a surprise due to the similarity between both antibiotics (Fig. 1). A concentration-dependent pattern has been described for other DNA-binding drugs (see [14] and references there in). This is clearly related to the nature of the ligand but also depends upon the nature of the DNA molecule (cf. Figs. 3 and 5). The concentration-dependence of the footprinting pattern is observed with the tyrT DNA (cf. Figs. 3 and 5) but it is more evident in other fragments as, for example, the 70-mer.

It has been reported that chartreusin would bind cooperatively to poly[d(AT)]·poly[d(AT)] and poly-[d(GC)]·poly[d(GC)] but not to calf thymus DNA [3]. An explanation given to these results suggested a 2–3 base-pair binding sites, with the antibiotic binding with high affinity to alternating AT and GC sites [3]. It is not possible to check the presence of cooperative binding, since the possibility of A+T or G+C protected sites appearing in long tracts is relatively small in the DNAs we have used in our footprinting study. Nonetheless, it is noteworthy that none of the AT-rich tracts found in these DNAs is significantly protected from DNase I cleavage. Unfortunately, no similar studies have been performed (to our knowledge) on the elsamicin binding to DNA polymers of different base-pair compositions, so we cannot compare our footprinting data in the same way. It is tempting to speculate whether the larger bind-

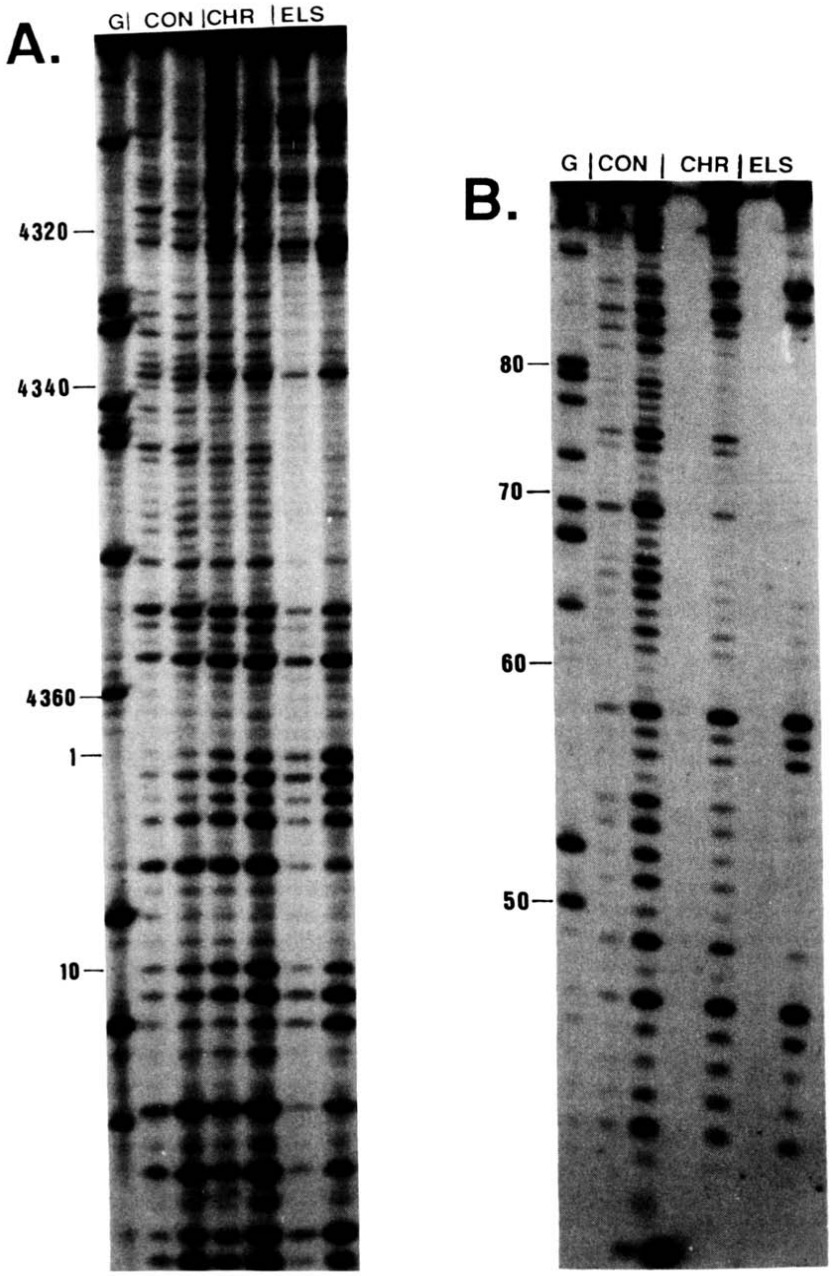

Fig. 5. DNase I footprinting of 30 μM chartreusin (CHR) and 15 μM elsamicin (ELS) on the 102-mer (*Aat*II-*Hin*dIII) (A) and 70-mer (*Hin*dIII-*Hha*I) (B) fragments from pBR322. Each set of two tracks represents 1 min and 5 min digestion by the enzyme. Other details as in legend to Fig. 3.

ing sites for elsamicin may reflect a cooperative behaviour in at least some of the binding sites. Although, at present, this explanation cannot be ruled out, we are more inclined to believe that the larger binding sites reflect a steric blockage of one extra base pair without direct binding, or even a quadruplet binding site for elsamicin. This might favour an extra hydrogen bridge involving the charged amino group of one of the sugar moieties and/or accommodate the extra methyl group of the neutral sugar (see Fig. 1). The low solubility of chartreusin does not allow the use of the hydroxyl radical as a footprinting tool since the presence of DMSO will quench the reaction. It is well known that only drugs which are soluble in aqueous solutions have been successfully footprinted using hydroxyl radicals [18,19]. A deeper knowledge of the characteristics of the binding sites and the specific contacts between the DNA bases and the disaccharide moieties of these antibiotics will require the availability of crystallised structures. Our footprinting results suggest the use of oligonucleotides containing a 5'-CG-3' step for this purpose.

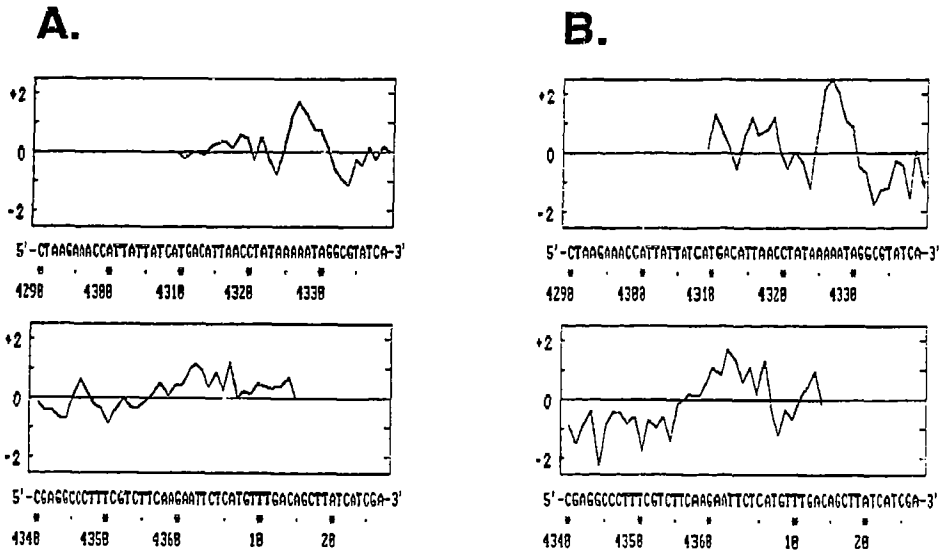

Fig. 6. Differential cleavage plot for the 102-mer fragment of pBR322 in the presence of chartreusin, 30 μM (A), and in the presence of elsamicin, 15 μM (B). Other details as in legend to Fig. 4.

Acknowledgements: This work was supported in part by a grant from the CICYT, Spain (SAL89-0038-CE) and the contract TS2-M-0026-E from the CEE.

REFERENCES

[1] Simonitsh, E., Eisenhuth, W., Stamm, O.A. and Schmid, H. (1964) Helv. Chim. Acta 47, 1459–1475.
[2] Konishi, M., Sugawara, K., Kotu, F., Nishiyama, Y., Tomita, K., Miyaki, T. and Kawaguchi, H. (1986) J. Antibiot. 39, 784–791.
[3] Krueger, W.C., Pschigoda, L.M. and Moscowitz, A. (1986) J. Antibiot. 39, 1298–1303.
[4] Sugawara, K., Tsunakawa, M., Konishi, M., Kawaguchi, H., Krishnan, B., Cunheng, H. and Clardy, J. (1987) J. Org. Chem. 52, 996–1001.
[5] McGovren, J.P., Neil, G.L., Crampton, S.L., Robinson, M.I. and Douros, J.D. (1977) Cancer Res. 37, 1666–1672.
[6] Gaver, R.C., Deeb, G. and George, A.M. (1989) Cancer Chemother. Pharmacol. 25, 195–201.
[7] Yagi, M., Nishimura, T., Suzuki, H. and Tanaka, N. (1981) Biochem. Biophys. Res. Commun. 98, 642–647.
[8] Uramoto, M., Kusano, T., Nishio, K., Isono, K., Shishido, K. and Ando, T. (1983) FEBS Lett. 153, 325–328.
[9] Shuring, J.E., Forenza, S., Long, B.H., Rose, W.C., Catino, J.J., Kamei, H., Nishiyama, Y., Bradner, W.H., Casazza, A.M., Stringfellow, D.A. and Doyle, T.W. (1988) Proc. Am. Assoc. Cancer Res. 29, 538–539.
[10] Portugal, J. (1989) Chem.-Biol. Interact. 71, 311–324.
[11] Drew, H.R. and Travers, A.A. (1984) Cell 37, 491–502.
[12] Low, C.M.L., Drew, H.R. and Waring, M.J. (1984) Nucleic Acids Res. 12, 4865–4879.
[13] Fox, K.R. and Waring, M.J. (1984) Nucleic Acids Res. 12, 9271–9285.
[14] Portugal, J. and Waring, M.J. (1987) Eur. J. Biochem. 167, 281–289.
[15] Fox, K.R. and Grigg, G.W. (1988) Nucleic Acids Res. 16, 2063–2075.
[16] Portugal, J., Fox, K.R., Mclean, M.J., Richenberg, J.L. and Waring, M.J. (1988) Nucleic Acids Res. 16, 3655–3670.
[17] Suck, D. and Oefner, C. (1986) Nature 321, 620–625.
[18] Portugal, J. and Waring, M.J. (1987) FEBS Lett. 225, 195–200.
[19] Cons, B.M.G. and Fox, K.R. (1989) Nucleic Acids Res. 17, 5447–5459.